TABLE 2. Acute hemodynamic changes

Variable	All		Mild		Moderate		Severe	
	Baseline (n = 46)	Discharge (n = 33)	Baseline (n = 19)	Discharge (n = 13)	Baseline (n = 17)	Discharge (n = 14)	Baseline (n = 10)	Discharge (n = 6)
LVEDVI (mL/m^2)	140 ± 38	110 ± 35*	129 ± 29	105 ± 22*	144 ± 45	106 ± 42*	155 ± 35	133 ± 41*
LVESVI (mL/m^2)	104 ± 34	59 ± 29*	94 ± 25	53 ± 17*	105 ± 40	54 ± 28*	120 ± 33	85 ± 40*
LVEF (%)	26 ± 7	37 ± 12*	27 ± 8	39 ± 10*	28 ± 7	38 ± 13*	23 ± 6	32 ± 16*
LVSP (mm Hg)	116 ± 22	120 ± 15	114 ± 19	120 ± 14	120 ± 20	121 ± 15	111 ± 29	118 ± 20
LVEDP (mm Hg)	20 ± 8	12 ± 4*	17 ± 8†	10 ± 3*	20 ± 5	14 ± 4*	26 ± 8	14 ± 5*
PCWP (mm Hg)	20 ± 8	15 ± 5*	16 ± 8†	13 ± 4	20 ± 6	16 ± 4	27 ± 8	17 ± 7
Systolic PAP (mm Hg)	44 ± 15	35 ± 8*	34 ± 10†	31 ± 7†	43 ± 10†	38 ± 8	59 ± 16	39 ± 10*
Mean PAP (mm Hg)	29 ± 10	23 ± 5*	22 ± 7†	20 ± 4†	29 ± 7†	25 ± 5	40 ± 10	26 ± 5*
RAP (mm Hg)	8.2 ± 4.5	8.9 ± 3.0	6.7 ± 3.8	8.0 ± 2.9	7.9 ± 4.8	9.7 ± 2.7	10.0 ± 4.2	9.0 ± 4.0
CI (L/min/m^2)	2.6 ± 0.6	3.0 ± 0.7*	2.6 ± 0.5	3.1 ± 0.7*†	2.7 ± 0.6	3.0 ± 0.7*†	2.2 ± 0.6	2.2 ± 0.4
TMPG (mm Hg)	0.4 ± 6.4	2.5 ± 3.1	0.1 ± 6.6	2.8 ± 3.1	0.2 ± 7.0	2.1 ± 2.9	1.4 ± 5.5	2.7 ± 3.7
SVR (dynes · s · cm^{-5})	1520 ± 380	1320 ± 420*	1590 ± 340	1310 ± 310*	1490 ± 470	1240 ± 290*	1470 ± 310	1520 ± 740
PVR (dynes · s · cm^{-5})	171 ± 90	137 ± 54	127 ± 62†	123 ± 44†	162 ± 48†	143 ± 63	243 ± 122	147 ± 53*

LVEDVI, Left ventricular end-diastolic volume index; *LVESVI,* left ventricular end-systolic volume index; *LVEF,* left ventricular ejection fraction; *PCWP,* pulmonary capillary wedge pressure; *PAP,* pulmonary artery pressure; *RAP,* right atrial pressure; *CI,* cardiac index; *TMPG,* transmitral pressure gradient; *SVR,* systemic vascular resistance; *PVR,* pulmonary vascular resistance. *$P < .05$ versus variables at baseline in each group. †$P < .05$ versus severe PH group at each point.

a decreased tenting height and adequate coaptation length. No significant differences were found postoperatively in the changes in MR grade, TR grade, coaptation length, tenting height, mitral valve orifice area, or mean transmitral pressure gradient among the 3 study groups.

Symptoms and Serum BNP Levels

The NYHA functional improvements and changes in serum BNP levels were not significantly associated with the preoperative severity of PH (Figure 5). The patients in the severe PH group tended to show less improvement. In

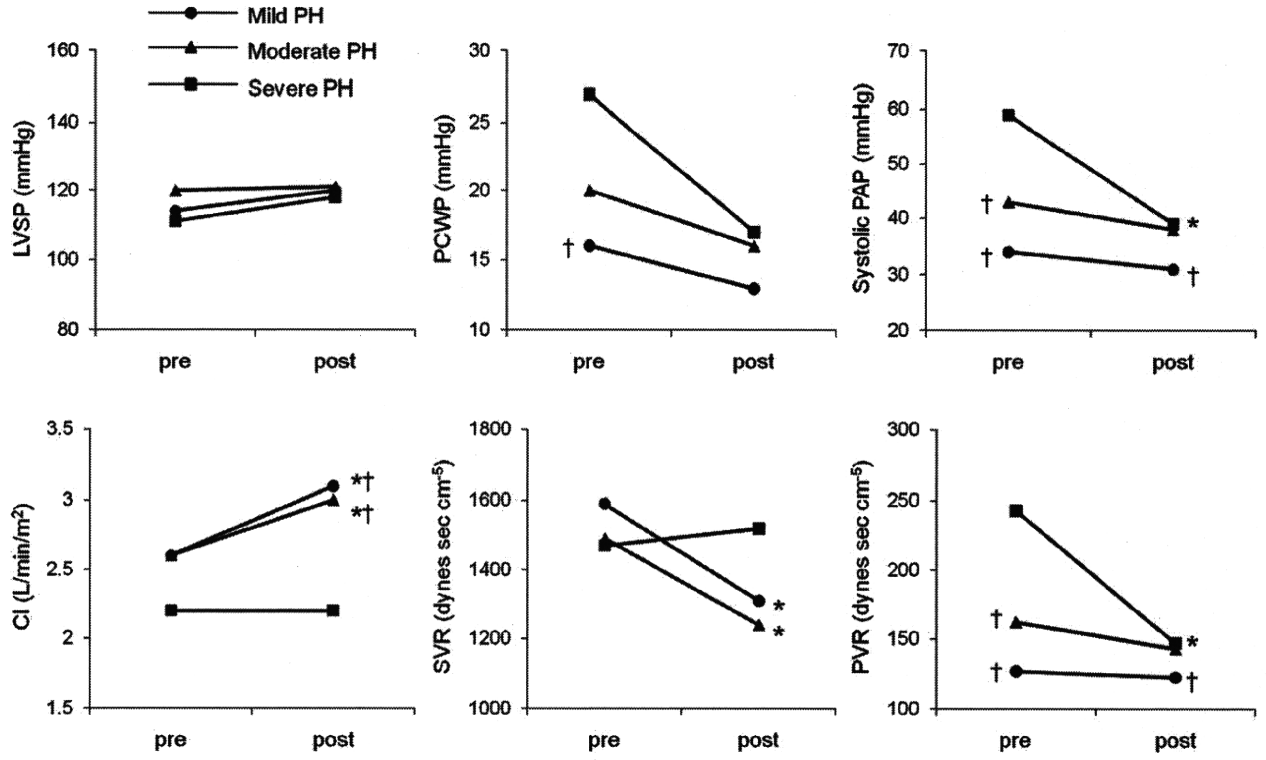

FIGURE 3. Acute hemodynamic changes after restrictive mitral annuloplasty. *$P < .05$ versus value at baseline, †$P < .05$ versus value for severe pulmonary hypertension *(PH)* group. *LVSP,* Left ventricular systolic pressure; *PCWP,* pulmonary capillary wedge pressure; *PAP,* pulmonary artery pressure; *CI,* cardiac index; *SVR,* systemic vascular resistance; *PVR,* pulmonary vascular resistance. *Circles, triangles,* and *squares* indicate mild, moderate, and severe groups, respectively.

TABLE 3. Serial echocardiographic and functional variables

Variable	Baseline	1 mo	1 y	2 y	*P* Value
LVEDD (mm)					
All	66 ± 6	60 ± 7*	60 ± 8*	59 ± 8*	< .01
Mild PH group	66 ± 6	58 ± 6*†	58 ± 9*	57 ± 9*	< .01
Moderate PH group	65 ± 6	58 ± 7*†	58 ± 5*	56 ± 4*	< .01
Severe PH group	69 ± 6	67 ± 6	66 ± 8	64 ± 10	NS
LVESD (mm)					
All	55 ± 7	48 ± 10*	45 ± 10*	44 ± 12*	< .01
Mild PH group	54 ± 7†	45 ± 8*†	42 ± 9*	40 ± 11*	< .01
Moderate PH group	53 ± 7†	46 ± 10*†	43 ± 10*	41 ± 6*	< .01
Severe PH group	61 ± 6	58 ± 7	52 ± 11	52 ± 13	NS
LVEF (%)					
All	32 ± 5	39 ± 8*	44 ± 7*	45 ± 7*	< .01
Mild PH group	34 ± 4†	42 ± 5*†	46 ± 7*†	49 ± 6*†	< .01
Moderate PH group	33 ± 6†	40 ± 10*†	45 ± 5*†	45 ± 5*†	< .01
Severe PH group	29 ± 4	31 ± 6	37 ± 9*	39 ± 8*	.02
LA dimension (mm)					
All	51 ± 7	45 ± 6*	48 ± 5*	48 ± 5*	< .01
Mild PH group	49 ± 6	44 ± 6*†	48 ± 5	47 ± 5	.03
Moderate PH group	51 ± 6	45 ± 3*	48 ± 5	49 ± 4	< .01
Severe PH group	52 ± 9	50 ± 7	50 ± 6	49 ± 8	NS
Systolic PAP (mm Hg)					
All	47 ± 15	36 ± 8*	38 ± 9*	37 ± 13*	< .01
Mild PH group	33 ± 4†	33 ± 6	32 ± 9	29 ± 9	NS
Moderate PH group	48 ± 6†	36 ± 7*	36 ± 8*	36 ± 10*	.02
Severe PH group	70 ± 9	42 ± 8*	50 ± 11*	54 ± 17	.01
MR grade					
All	3.6 ± 0.5	0.9 ± 0.7*	0.9 ± 0.7*	1.0 ± 0.7*	< .01
Mild PH group	3.6 ± 0.5	0.8 ± 0.4*	0.8 ± 0.7*	0.8 ± 0.6*	< .01
Moderate PH group	3.6 ± 0.5	0.9 ± 0.7*	0.8 ± 0.6*	1.0 ± 0.0*	< .01
Severe PH group	3.8 ± 0.5	1.3 ± 1.2*	1.0 ± 0.9*	1.3 ± 1.0*	.02
TR grade					
All	2.3 ± 1.1	0.9 ± 0.6*	0.9 ± 0.6*	1.0 ± 0.6*	< .01
Mild PH group	2.3 ± 1.2	0.8 ± 0.7*	0.8 ± 0.6*	1.0 ± 0.0*	< .01
Moderate PH group	2.2 ± 1.0	0.8 ± 0.4*	0.8 ± 0.4*	1.2 ± 0.8*	.02
Severe PH group	2.5 ± 1.3	1.1 ± 0.6*	1.3 ± 0.7*	1.2 ± 0.4*	.03
Tenting height (mm)					
All	7.9 ± 2.4	4.2 ± 1.9*	3.8 ± 0.9*	4.0 ± 1.4*	< .01
Mild PH group	6.7 ± 2.3	4.7 ± 2.2*	4.0 ± 1.1*	3.6 ± 0.4*	< .01
Moderate PH group	8.0 ± 2.0	3.7 ± 1.2*	3.6 ± 0.7*	4.3 ± 2.0*	< .01
Severe PH group	10.1 ± 1.7	4.1 ± 2.3*	3.8 ± 0.8*	4.2 ± 0.3*	< .01
Coaptation length (mm)					
All	4.1 ± 1.5	8.0 ± 2.4*	8.2 ± 1.1*	7.9 ± 1.1*	< .01
Mild PH group	4.4 ± 1.7	7.4 ± 1.8*	8.1 ± 1.4*	8.0 ± 1.3*	< .01
Moderate PH group	4.2 ± 1.5	8.7 ± 3.0*	8.2 ± 1.0*	7.9 ± 1.0*	< .01
Severe PH group	3.0 ± 0.7	7.9 ± 2.0*	8.3 ± 1.3*	7.7 ± 1.3*	< .01
Effective orifice area (cm^2)					
All		2.6 ± 0.3	2.6 ± 0.4	2.5 ± 0.4	NS
Mild PH group		2.6 ± 0.3	2.6 ± 0.3	2.5 ± 0.3	NS
Moderate PH group		2.6 ± 0.4	2.6 ± 0.3	2.5 ± 0.3	NS
Severe PH group		2.6 ± 0.4	2.7 ± 0.4	2.6 ± 0.4	NS

(Continued)

contrast, in the mild and moderate PH groups, the NYHA functional class improved significantly, and the improvement persisted during the follow-up period, along with reduced serum BNP levels.

Prediction for Reverse LV Remodeling

When substantial reverse LV remodeling was defined as a 10% reduction in the LVEDD, LV reverse remodeling was seen in 16 (89%) of 18 patients with mild PH, 12

TABLE 3. Continued

Variable	Baseline	1 mo	1 y	2 y	*P* Value
TMPG (mm Hg)					
All		4.2 ± 1.5	4.3 ± 1.6	4.7 ± 2.3	NS
Mild PH group		4.7 ± 1.6	4.6 ± 1.3	4.9 ± 2.0	NS
Moderate PH group		3.7 ± 1.3	3.9 ± 1.3	4.7 ± 2.1	NS
Severe PH group		4.4 ± 1.4	4.5 ± 2.6	4.5 ± 3.4	NS

LVEDD, left ventricular end-diastolic dimension; *PH*, pulmonary hypertension; *LVESD*, left ventricular end-systolic dimension; *LVEF*, left ventricular ejection fraction; *LA*, left atrial; *PAP*, pulmonary artery pressure; *MR*, mitral regurgitation; *TR*, tricuspid regurgitation; *TMPG*, transmitral pressure gradient. *$P < .05$ versus values at baseline in each group. †$P < .05$ versus severe PH group at each point.

(71%) of 17 patients with moderate PH, and 2 (25%) of 8 with severe PH (P = NS) at their most recent examination (Table 4). Univariate analysis identified LV systolic dysfunction (P = .022), a longer duration of heart failure (P = .01), and severe PH (systolic PAP > 60 mm Hg; P = .004) as important predictors of failure of reverse LV remodeling. In addition, multivariate analysis identified severe PH as a significant predictor.

Prediction of Postoperative Adverse Cardiac Events

Finally, the potential predictors of postoperative adverse cardiac events were examined using a Cox proportional hazard model (Table 5). Univariate analysis identified preoperative LV systolic dysfunction (P = .04), a longer duration of heart failure (P = .021), and severe PH (systolic PAP > 60 mm Hg; P = .002) as important predictors. In addition, multivariate analysis identified severe PH as a significant predictor.

DISCUSSION

The results of the present study suggest that PH in patients with advanced cardiomyopathy undergoing RMA is significantly associated with adverse short-term clinical outcome in terms of overall survival, adverse cardiac events (including cardiac death, readmission for heart failure, and fatal arrhythmia), improvements in NYHA functional class and serum BNP levels, acute hemodynamic changes, and serial echocardiographic changes in LV dimensions and function. Our findings have also demonstrated that severe PH (systolic PAP > 60 mm Hg) was an important hemodynamic predictor of adverse cardiac events, as well as failure of LV reverse remodeling after surgical treatment for functional MR and LV dysfunction.

In previous studies, clinical variables such as advanced age, preoperative hemodialysis and diabetes,[4] larger LV dimensions,[5,6] and nonischemic etiology and a longer duration of heart failure[7] were shown to be significantly associated with poor outcomes after RMA. In addition, the more sophisticated echocardiographic parameters of LV systolic and diastolic dysfunction such as LVEDD (> 65 mm) and left ventricular end-systolic dimension (> 51 mm),[8] myocardial performance index, systolic sphericity, wall motion score index,[14,15] restrictive LV filling

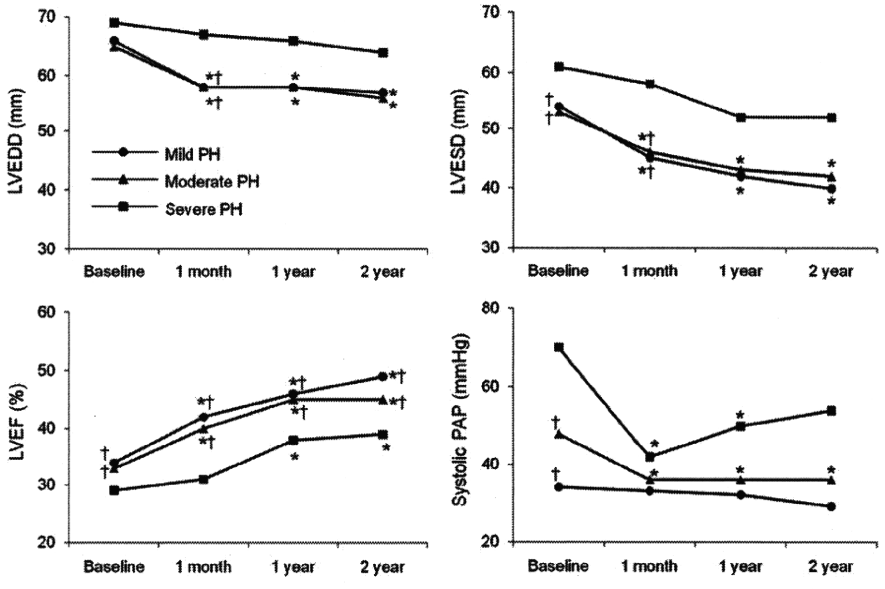

FIGURE 4. Serial echocardiographic changes after restrictive mitral annuloplasty. *$P < .05$ versus value at baseline, †$P < .05$ versus value for severe PH group. *LVEDD*, Left ventricular end-diastolic dimension; *LVEF*, left ventricular ejection fraction; *LVESD*, left ventricular end-systolic dimension; *PAP*, pulmonary artery pressure; *PH*, pulmonary hypertension.

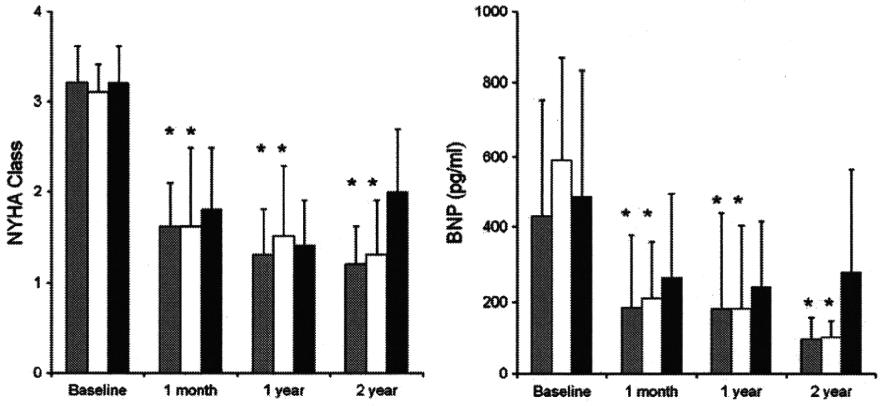

FIGURE 5. Serial changes in New York Heart Association *(NYHA)* functional class and serum brain natriuretic peptide *(BNP)* level. *$P < .05$ versus value at baseline. *Gray*, *white*, and *black* bars indicate mild, moderate, and severe groups, respectively.

pattern and mitral deceleration time (< 140 ms)[16] have been reported to be strong predictors of poor outcome or a lack of LV reverse remodeling after RMA. These parameters have also been shown to predict late MR recurrence after mitral annuloplasty. The present results have suggested that the PH level is a strong predictor of outcome after RMA and also provided additional important prognostic information that is complementary to the classic echocardiographic parameters of LV systolic and diastolic dysfunction.

The etiologies of PH in patients with cardiomyopathy are heterogeneous, and the determinants of its reversibility after an annuloplasty procedure have not been fully clarified. Classically, PH in patients with cardiomyopathy has been attributed to elevated LV filling pressures, reactive pulmonary arterial vasoconstriction, pulmonary vascular remodeling, or all three[17]; it has also been associated with functional MR.[18] The increased PAP associated with early-stage cardiomyopathy principally results from elevated LV filling pressures.[18] In addition, longstanding elevation of LV filling pressures can lead to several histologic changes in pulmonary circulation, including medial hypertrophy of arterioles, intimal fibroproliferation, and arterialization of the pulmonary veins.[17] These changes have also been associated with neurohumoral activation, in particular of endothelin-1,[19,20] a potent vasoconstrictor that is markedly increased in patients with advanced heart failure. These pathophysiologic changes are dependent on the chronicity and severity of PH and can initially be reversible, although the conditions can eventually become irreversible.[17]

The changes in pulmonary hemodynamics seen in the present severe PH group were consistent with this sequence of PH progression. The patients in the severe PH group had had a longer duration of heart failure and greater PVR values before surgery. Furthermore, the mean PVR value in this group remained considerably elevated at 1 month

TABLE 4. Predictors of failure in left ventricular reverse remodeling

	Univariate			Multivariate		
Variable	*P* Value	Odds Ratio	95% CI	*P* Value	Odds Ratio	95% CI
Age	NS					
Ischemic etiology	NS					
Duration of HF	.01	1.1	1.02–1.15	NS		
History of VT	NS					
LVEDD (continuous)	NS					
LVEDD (> 65 mm)	NS					
LVESD (continuous)	NS					
LVESD (> 50 mm)	NS					
LA dimension (mm)	NS					
LVEF (%)	.02	0.8	0.70–0.97	NS		
Severe PH*	.004	25.7	4.3–155	.03	10.0	1.3–75
MR grade	NS					
TR grade	NS					

CI, Confidence interval; *HF*, heart failure; *VT*, ventricular tachycardia; *LVEDD*, left ventricular end-diastolic dimension; *LVESD*, left ventricular end-systolic dimension; *LA* , left atrial; *LVEF*, left ventricular ejection fraction; *PH*, pulmonary hypertension; *MR*, mitral regurgitation; *TR*, tricuspid regurgitation. *Systolic PAP > 60 mm Hg.

TABLE 5. Predictors of adverse cardiac events

	Univariate			Multivariate		
Variable	*P* Value	Hazard Ratio	95% CI	*P* Value	Hazard Ratio	95% CI
Age	NS					
Ischemic etiology	NS					
Duration of HF	.02	1.05	1.01–1.10	NS		
History of VT	NS					
LVEDD (continuous)	NS					
LVEDD (> 65 mm)	NS					
LVESD (continuous)	NS					
LVESD (> 50 mm)	NS					
LA dimension (mm)	NS					
LVEF (%)	.04	0.89	0.79–0.96	NS		
Severe PH*	.002	9.1	2.3–35	.04	6.9	1.1–44
MR grade	NS					
TR grade	NS					

CI, Confidence interval; *HF*, heart failure; *VT*, ventricular tachycardia; *LVEDD*, left ventricular end-diastolic dimension; *LVESD*, left ventricular end-systolic dimension; *LA*, left atrial; *LVEF*, left ventricular ejection fraction; *PH*, pulmonary hypertension; *MR*, mitral regurgitation; *TR*, tricuspid regurgitation. *Systolic PAP > 60 mm Hg.

after surgery. The elevated PAP levels (> 40 mm Hg) persisted at all follow-up examinations, suggesting the presence of irreversible pulmonary vascular disease. In contrast, the moderate PH group showed a decline in the systolic PAP without a change in the lowered PVR at discharge. Also, the lower PAP values were maintained until the latest follow-up examination, suggesting that PH was reversible in these patients. Thus, our findings emphasize the importance of assessing PVR and the degree of pulmonary vascular remodeling. In addition, our results might support the use of surgery for patients with medically uncontrollable severe functional MR before the pulmonary vascular disease becomes irreversible.

The degree of PH is not only related to the severity of LV systolic dysfunction, but is also strongly associated with the LV diastolic dysfunction (i.e., a greater level of PH has been associated with a shorter mitral deceleration time).[18] Gelsomino and colleagues[21] reported that the Doppler-derived mitral deceleration time was prognostic for LV reverse remodeling after undersized mitral annuloplasty. Our results are not necessarily inconsistent with those of previous studies, because a strong correlation between the Doppler-derived systolic PAP and mitral deceleration time has been reported.[18] Also, the prevalence of a restrictive filling pattern has been inversely related to the LVEF. PH has also been significantly associated with right ventricular function and right heart hemodynamics. In contrast, the right ventricular EF will correlate with the systolic PAP and is an independent predictor of survival in patients with moderate heart failure.[22] This association between PH and right ventricular dysfunction could explain why the level of PH provides additional prognostic information beyond the LV systolic and diastolic dysfunction variables.

It remains controversial whether patients with end-stage heart failure and functional MR can benefit from RMA.[23-25] In our study, patients with mild and moderate PH (Doppler-derived PAP < 60 mm Hg) showed functional improvement and satisfactory long-term survival. In contrast, those with severe PH (systolic PAP > 60 mm Hg) had relatively poor outcomes. Our results have shown that RMA was able to improve hemodynamics and symptoms in these patients. However, the lack of an untreated control group did not allow us to investigate the survival benefit conferred by RMA for patients with significant MR and severe LV dysfunction. Additional studies of late mortality after RMA in similar patient populations are needed.

Study Limitations

The main limitations of the present study were its retrospective nature and the small number of subjects. The inclusion of patients with ischemic and nonischemic cardiomyopathy and those who had undergone concomitant coronary artery bypass grafting, tricuspid annuloplasty, and a maze procedure for atrial fibrillation might have influenced the results. However, these concomitant procedures are usually required in a population of very sick patients who present with similar clinical and pathophysiologic status despite the etiology of LV dysfunction. To minimize the potential bias related to patient selection, our study population consisted only of patients with advanced nonischemic or ischemic cardiomyopathy owing to anterior infarction and functional MR. Patients with less LV remodeling and ischemic MR secondary to predominant inferior/posterior infarction, who have often been included in previous studies,[6-8,15,16,21,24] were excluded from our study. Therefore, our results would not be applicable to patients with previous inferior or lateral infarction.

During the late follow-up examinations, systolic PAP was determined noninvasively using Doppler echocardiography and not measured by catheterization. This noninvasive method has been fully validated and currently represents a standard approach for PH determination. In the present study, we confirmed that systolic PAP estimated using Doppler echocardiography correlated significantly with the nonsimultaneously catheter-derived systolic PAP ($r = .833$, $P < .001$). Moreover, Bland-Altman analysis showed that the 2 modalities had good agreement in the measurements of systolic PAP, although it was slightly overestimated using Doppler echocardiography (mean bias 1.5 ± 8.4 mm Hg).

The medical treatments administered could have also affected our findings. However, the preoperative medical therapies were continued without significant modifications after surgical intervention. In particular, the use and dosage of angiotensin-converting enzyme inhibitors and angiotensin-II receptor blockers were not changed; thus, their influence on LV remodeling and pulmonary vascular remodeling in our patients was considered to be negligible.

CONCLUSIONS

Noninvasive assessment of systolic PAP was found to be an excellent prognostic tool for patients who underwent RMA for functional MR secondary to advanced cardiomyopathy. Additional studies are needed to define the mechanism of PH and its postoperative reversibility in patients with cardiomyopathy to establish new treatment strategies.

The authors thank Kiyoshi Yoshida, CE, and Shin-ichi Fujita for their data collection in regard to surgical intervention and echocardiographic findings. We also thank Hiroyuki Waki for his assistance with the statistical analysis.

References

1. Abramson SV, Burke JF, Kelly JJ Jr, Kitchen JG III, Dougherty MJ, Yih DF, et al. Pulmonary hypertension predicts mortality and morbidity in patients with dilated cardiomyopathy. *Ann Intern Med.* 1992;116:888-95.
2. Costard-Jäckle A, Fowler MB. Influence of preoperative pulmonary artery pressure on mortality after heart transplantation: testing of potential reversibility of

pulmonary hypertension with nitroprusside is useful in defining a high risk group. *J Am Coll Cardiol.* 1992;19:48-54.
3. Bolling SF, Deeb GM, Brunsting LA, Bach DS. Early outcome of mitral valve reconstruction in patients with end-stage cardiomyopathy. *J Thorac Cardiovasc Surg.* 1995;109:676-83.
4. Crabtree TD, Bailey MS, Moon MR, Munfakh N, Pasque MK, Lawton JS, et al. Recurrent mitral regurgitation and risk factors for early and late mortality after mitral valve repair for functional ischemic mitral regurgitation. *Ann Thorac Surg.* 2008;85:1537-42.
5. Szalay ZA, Civelek A, Hohe S, Brunner-LaRocca HP, Klövekorn WP, Knez I, et al. Mitral annuloplasty in patients with ischemic versus dilated cardiomyopathy. *Eur J Cardiothorac Surg.* 2003;23:567-72.
6. Bax J, Braun J, Somer ST, Klautz R, Holman ED, Versteegh MIM, et al. Restrictive annuloplasty and coronary revascularization in ischemic mitral regurgitation results in reverse left ventricular remodeling. *Circulation.* 2004;110(Suppl II): II-103-8.
7. De Bonis M, Lapenna E, Verzini A, La Canna G, Grimaldi A, Torracca L, et al. Recurrence of mitral regurgitation parallels the absence of left ventricular reverse remodeling after mitral repair in advanced dilated cardiomyopathy. *Ann Thorac Surg.* 2008;85:932-9.
8. Braun J, van de Veire NR, Klautz RJM, Versteegh MIM, Holman ER, Westenberg JJM, et al. Restrictive mitral annuloplasty cures ischemic mitral regurgitation and heart failure. *Ann Thorac Surg.* 2008;85:430-7.
9. Nagueh SF, Kopelen HA, Zoghbi WA. Relation of mean right atrial pressure to echocardiographic and Doppler parameters of right atrial and right ventricular function. *Circulation.* 1996;93:1160-9.
10. Pepi M, Tamborini G, Galli C, Barbier P, Doria E, Berti M, et al. A new formula for echo-Doppler estimation of right ventricular systolic pressure. *J Am Soc Echocardiogr.* 1994;7:20-6.
11. Kircher BJ, Himelman RB, Schiller NB. Noninvasive estimation of right atrial pressure from the inspiratory collapse of the inferior vena cava. *Am J Cardiol.* 1990;66:493-6.
12. Taniguchi K, Nakano S, Kawashima Y, Sakai K, Kawamoto T, Sakaki S, et al. Left ventricular ejection performance, wall stress, and contractile state in aortic regurgitation before and after aortic valve replacement. *Circulation.* 1990;82: 798-807.
13. Bland JM, Altman DG. Statistical methods for assessing agreement between two methods of clinical measurement. *Lancet.* 1986;1:307-10.
14. Tei C, Ling LH, Hodge DO, Bailey KR, Oh JK, Rodeheffer RJ, et al. New index of combined systolic and diastolic myocardial performance: a simple and reproducible measure of cardiac function—a study in normals and dilated cardiomyopathy. *J Cardiol.* 1995;26:357-66.
15. Gelsomino S, Lorusso R, Capecchi I, Rostagno C, Romagnoli S, Billè G, et al. Left ventricular reverse remodeling after undersized mitral ring annuloplasty in patients with ischemic regurgitation. *Ann Thorac Surg.* 2008;85:1319-30.
16. Gelsomino S, Lorusso R, Billè G, Rostagno C, De Cicco G, Romagnoli S, et al. Left ventricular diastolic function after restrictive mitral ring annuloplasty in chronic ischemic mitral regurgitation and its predictive value on outcome and recurrence of regurgitation. *Int J Cardiol.* 2009;132:419-28.
17. Delgado JF, Conde E, Sánchez V, López-Ríos F, Gómez-Sánchez MA, Escribano P, et al. Pulmonary vascular remodeling in pulmonary hypertension due to chronic heart failure. *Eur J Heart Fail.* 2005;7:1011-6.
18. Enriquez-Sarano M, Rossi A, Seward JB, Bailey KR, Tajik AJ. Determinants of pulmonary hypertension in left ventricular dysfunction. *J Am Coll Cardiol.* 1997; 29:153-9.
19. Cody RJ, Haas GJ, Binkley PF, Capers Q, Kelley R. Plasma endothelin correlates with the extent of pulmonary hypertension in patients with chronic congestive heart failure. *Circulation.* 1992;85:504-9.
20. Moraes DL, Colucci WS, Givertz MM. Secondary pulmonary hypertension in chronic heart failure: the role of the endothelium in pathophysiology and management. *Circulation.* 2000;102:1718-23.
21. Gelsomino S, Lorusso R, Rostagno C, Caciolli S, Billè G, De Cicco G, et al. Prognostic value of Doppler-derived mitral deceleration time on left ventricular reverse remodelling after undersized mitral annuloplasty. *Eur J Echocardiogr.* 2008;9:631-40.
22. de Groote P, Millaire A, Foucher-Hossein C, Nugue O, Marchandise X, Ducloux G, et al. Right ventricular ejection fraction is an independent predictor of survival in patients with moderate heart failure. *J Am Coll Cardiol.* 1998;32: 948-54.
23. Wu AH, Aaronson KD, Bolling SE, Pagani FD, Welch K, Koelling TM. Impact of mitral valve annuloplasty on mortality risk in patients with mitral regurgitation and left ventricular systolic dysfunction. *J Am Coll Cardiol.* 2005;45:381-7.
24. Fattouch K, Guccione F, Sampognaro R, Panzarella G, Corrado E, Navarra E, et al. POINT: efficacy of adding mitral valve restrictive annuloplasty to coronary artery bypass grafting in patients with moderate ischemic mitral valve regurgitation: a randomized trial. *J Thorac Cardiovasc Surg.* 2009;138:278-85.
25. Trento A, Goland S, De Robertis MA, Czer LS. COUNTERPOINT: efficacy of adding mitral valve restrictive annuloplasty to coronary artery bypass grafting in patients with moderate ischemic mitral valve regurgitation. *J Thorac Cardiovasc Surg.* 2009;138:286-8.

ACD

APPENDIX

The following variables were tested: age, gender, body surface area, NYHA functional class, ischemic etiology, hypertension, diabetes, hyperlipidemia, chronic obstructive pulmonary disease, chronic renal failure, peripheral vascular disease, cerebral vascular disease, atrial fibrillation, history of ventricular arrhythmia, duration of heart failure (in months), multivessel coronary artery disease, previous coronary artery bypass grafting, previous percutaneous coronary intervention, β-blockers, angiotensin-converting enzyme inhibitors, angiotensin-II receptor blocker, diuretics, LVEDD (continuous), LVEDD (>65 mm), left ventricular end-systolic dimension (continuous), left ventricular end-systolic dimension (> 50 mm), left atrial dimension, LVEF, tenting height, coaptation length, MR grade, TR grade, systolic PAP (continuous), and severe PH (systolic PAP > 60 mm Hg).

000 Pulmonary hypertension predicts adverse cardiac events after restrictive mitral annuloplasty for severe functional mitral regurgitation

Satoshi Kainuma, MD, Kazuhiro Taniguchi, MD, PhD, Koichi Toda, MD, PhD, Toshihiro Funatsu, MD, PhD, Haruhiko Kondoh, MD, PhD, Masami Nishino, MD, PhD, Takashi Daimon, PhD, and Yoshiki Sawa, MD, PhD, Osaka and Hyogo, Japan

We investigated the prognostic role of pulmonary hypertension in patients undergoing restrictive mitral annuloplasty for severe functional mitral regurgitation and found that pulmonary hypertension is an excellent prognostic tool for such patients. In particular, severe pulmonary hypertension (systolic pulmonary artery pressure > 60 mm Hg) was shown to be a predictor of adverse cardiac events and cardiac remodeling.

Editorial Manager(tm) for In Vitro Cellular & Developmental Biology - Animal
Manuscript Draft

Manuscript Number:

Title: Induction of enamel matrix protein expression in an ameloblast cell line co-cultured with a mesenchymal cell line in vitro

Article Type: Articles (full research papers)

Keywords: ameloblastin; tooth differentiation; co-culture

Corresponding Author: Prof.Dr. Akiyoshi Taniguchi, Ph.D.

Corresponding Author's Institution: National Institute for Materials Science

First Author: Asako Matsumoto

Order of Authors: Asako Matsumoto; Hidemitsu Harada, Ph.D. DDS; Masahiro Saito, Ph.D. DDS; Akiyoshi Taniguchi, Ph.D.

Abstract: Interactions between epithelium and mesenchyme are important for organ and tissue development. In this study, in order to mimic interactions between epithelium and mesenchyme during native tooth development, we constructed three-dimensional culture systems in vitro using a collagen membrane. Two types of collagen membrane-based in vitro culture systems were constructed in which dental epithelial and dental follicle cell lines were cultured. One co-culture method involved inoculation of one cell line into one side of the collagen membrane, and the other cell line into the opposite side of the membrane (sandwich co-culture; SW). As a control, the second method involved culture of one of the cell lines on a culture dish and the second cell line on a collagen membrane, facing away from the first cell line (separate co-culture; SC). The HAT-7 cells were also grown as a monolayer culture on collagen. Ameloblast differentiation in these cultures was investigated by analysis of the mRNA and/or protein expression of ameloblastin and amelogenin. Our results suggest that interaction of epithelial and mesenchymal cells via the extracellular matrix is important for tooth differentiation in vitro. Our culture system should be a useful method for investigation of epithelial-mesenchymal interactions.

Induction of enamel matrix protein expression in an ameloblast cell line co-cultured with a mesenchymal cell line *in vitro*

Asako Matsumoto[1,2,3], Hidemitsu Harada[4], Masahiro Saito[5] and Akiyoshi Taniguchi[1,2]

[1]Advanced Medical Materials Group, Biomaterials Center, National Institute for Materials Science, 1-1 Namiki, Tsukuba, Ibaraki 305-0044, Japan

[2]Biomaterials and Tissue Engineering, Graduate School of Comprehensive Human Science, University of Tsukuba, Tsukuba, Ibaraki 305-8572, Japan

[3]Kyokuto Pharmaceutical Industrial Co., Ltd. 3333-26 Aza-Asayama, Kamitezuna, Takahagi-shi, Ibaraki 318-0004, Japan

[4]Department of Oral Structure and Function Biology, Iwate Medical University, School of Dentistry, 1-3-27 Chuodori, Morioka, Iwate 020-8505, Japan

[5]Tissue Engineering Research Center, Tokyo University of Science, Noda, Chiba 278-8510, Japan

Keywords: ameloblastin, amelogenin, tooth differentiation, co-culture, ECM

Correspondence to: Akiyoshi Taniguchi

Biomaterials Center, National Institute for Materials Science, 1-1 Namiki, Tsukuba, Ibaraki 305-0044, Japan

Phone: +81-29-860-4505; Fax: +81-29-860-4714; E-mail: TANIGUCHI.Akiyoshi @nims.go.jp

Summary

Interactions between epithelium and mesenchyme are important for organ and tissue development. In this study, in order to mimic interactions between epithelium and mesenchyme during native tooth development, we constructed three-dimensional culture systems *in vitro* using a collagen membrane. Two types of collagen membrane-based *in vitro* culture systems were constructed in which dental epithelial and dental follicle cell lines were cultured. One co-culture method involved inoculation of one cell line into one side of the collagen membrane, and the other cell line into the opposite side of the membrane (sandwich co-culture; SW). As a control, the second method involved culture of one of the cell lines on a culture dish and the second cell line on a collagen membrane, facing away from the first cell line (separate co-culture; SC). The HAT-7 cells were also grown as a monolayer culture on collagen. Ameloblast differentiation in these cultures was investigated by analysis of the mRNA and/or protein expression of ameloblastin and amelogenin. Our results suggest that interaction of epithelial and mesenchymal cells via the extracellular matrix is important for tooth differentiation *in vitro*. Our culture system should be a useful method for investigation of epithelial-mesenchymal interactions.

Introduction

Epithelial cells communicate with epidermal cells through the extracellular matrix (ECM) to maintain and regulate highly differentiated functions. These interactions are thought to play an important role in the control of various characteristics of cells such as proliferation and differentiation. In order to mimic these interactions that occur in native tissue, three-dimensional culture systems have been created using various cell populations (Kurosawa et al. 2005; Ohno et al. 2008; Takayama et al. 2007) and reconstituted ECM (Takezawa et al. 2007). Co-culture models *in vitro* between two different cell types via reconstituted ECM have been developed for clarification of cell behavior associated with development, differentiation, regeneration, and pathogenesis *in vitro* (Gingras et al. 2003).

Tooth development is a classic instance of the process of epithelium-mesenchyme interactions and provides a useful experimental system for understanding the molecular mechanisms of organogenesis (Jernvall et al. 2000; Thesleff and Sharpe 1997). The early stage of tooth development is regulated by reciprocal interactions between epithelial and mesenchymal cells via cytokines such as transforming growth factor beta (TGFβ), fibroblast growth factor (FGF), and Leucine-Rich Amelogenin Protein (LRAP) [reviewed by (Thesleff and Mikkola 2002)], (Aberg et al. 1997; Thesleff and Mikkola 2002). Mesenchyme differentiates into odentoblasts which then form dentin. Epithelium differentiates into ameloblasts which secrete enamel matrix and form enamel. In the presecretory stage of tooth development, the dental epithelium and mesenchymal preodontoblasts are separated by the basement membrane matrix. [reviewed by (Thesleff and Hurmerinta 1981)].

Enamel matrix secreted by ameloblasts has been classified into two major

categories: amelogenin which makes up about 90% of the enamel extracellular matrix, and nonamelogenin including ameloblastin, enamelin, and tuftelin [reviewed by (Smith 1998)]. Ameloblastin, also known as amelin (Cerny et al. 1996) or sheathlin (Hu et al. 1997), and amelogenin are tooth-specific genes which play a critical role in proper tooth enamel formation (Fong et al. 1996; Fukumoto et al. 2004; Krebsbach et al. 1996; Xu et al. 2006a; Xu et al. 2006b). *In vitro* culture models that facilitate the study of epithelium-mesenchyme interactions are important for understanding tooth development at a molecular level. However, there is no useful model available that permits investigation of the molecular mechanism by which the ECM at sites of epithelial-mesenchymal interactions modulates tooth formation *in vitro*.

Collagen gels and matrigel often play important roles as scaffolds for reconstructing co-culture models. For example, endothelial cells form a network of branching tubular capillary-like structures into an overlaid collagen gel with embedded fibroblasts (Velazquez et al. 2002). The use of transparent collagen membranes has a number of advantages. It allows observation of the cells using a phase-contrast microscope, it can store cytokines and it is a simple culture method for three-dimensional culture systems (Orisaka et al. 2006).

In this study, we constructed three-dimensional culture systems *in vitro* using a collagen membrane for the co-culture of dental epithelial cells and dental follicle cells and gene and protein expression levels in these co-cultures were examined. Our results suggest that the interaction of epithelial and mesenchymal cells via the extracellular matrix is important for tooth differentiation *in vitro*.

Material and methods

Cells and Cell Cultures

The HAT-7 cells used in this study were derived from a dental epithelial cell line, which originated from the apical bud of a rat incisor (Kawano et al. 2002). The culture medium consisted of Dulbecco's modified Eagle's medium/F-12 (Invitrogen, Carlsbad, CA, USA) supplemented with 10% fetal bovine serum (FBS) and penicillin (100 units/ml)/streptomycin (100 μg/ml). The BCPb8 cells used were derived from a dental follicle cell line (a cementoblast progenitor), which originated from the follicle tissue of a bovine incisor (Saito et al. 2005). The culture medium consisted of α-minimum essential medium (α-MEM) supplemented with 10% FBS, penicillin (100 units/ml)/streptomycin (100 μg/ml), 50 mg/ml ascorbic acid and 2 mM L-glutamine (Invitrogen). All cultures were maintained in a humidified atmosphere of 5% CO_2 at 37 °C.

Co-culture using a transparent collagen membrane

Two different co-culture models were set up, both of which used the two dental cell lines and a transparent collagen membrane (Fig. 1). In the sandwich co-culture (SW) system one cell line was inoculated into one side of the collagen film in a culture dish and the second cell line was inoculated into the opposite side of the collagen film. (Orisaka et al. 2006). In the separate co-culture (SC) system, the BCPb8 cells were first seeded onto a 60 mm dish. After confirming microscopically that the BCPb8 cells had adhered to the dish, the dish and the transparent collagen membranes were washed with PBS. The HAT-7 cells (1×10^6 cells) were then seeded onto the collagen film inserted into the dish, on the side of the film facing away from the BCPb8 cells. The cells were

cultured in DMEM/F12 using 6.5 ml of medium per dish. The media were replaced with fresh media every two days. As a further control, HAT-7 cells were also grown in monolayer culture on a collagen film.

RNA Extraction and Real Time PCR Analysis

The mRNA levels of differentiation-related marker genes were determined using quantitative real-time PCR and species-specific primers (Kurosawa et al. 2005). Briefly, total RNA was extracted at various time points using ISOGEN (Nippon Gene, Tokyo, Japan). Three micrograms of total RNA was reverse-transcribed into cDNA using the SuperScript first-strand synthesis system (Invitrogen) according to the manufacturer's protocol.

Real-time PCR was performed using an ABI PRISM 7000 Sequence Detection System (Applied Biosystems, Foster City, CA, USA). A standard reaction was performed in a 96-well plate. This reaction was composed of 10 μl of SYBR Premix Ex TaqTM II (Takara, Siga, Japan), 10 pmol each of the forward and reverse primers, 1 μl of HAT-7 cDNA and distilled water to a final volume of 20 μl. The thermocycling conditions were 95 °C for 30 s, following by 40 cycles of 95 °C for 5 s and 60 °C for 34 s. Species-specific primers corresponding to a region of low-homology between rat and bovine cDNA were designed using Primer Express Software version 2.0 (Applied Biosystems) based on the sequence of the target gene. The data were normalized using expression of the housekeeping gene glyceraldehyde-3-phosphate dehydrogenase (GAPDH) as an endogenous control in the same reaction as the gene of interest. The primers used in this study were designated as follows: rat ameloblastin forward primer 5'-TTCACCCAAGGGAGGAGACTT-3, rat ameloblastin reverse primer

5'-CTCTCCTTTCTCAGGGCCTTTAGT-3', rat amelogenin forward primer 5'-TGGGAGCCCTGGTTATATCAA-3', rat amelogenin reverse primer 5'-GCTGCCTTATCATGCTCTGGT-A-3', rat GAPDH forward primer 5'-GCCCCCAACACTGAGCAT-3', rat GAPDH reverse primer, 5'-CCAGGCCCCTCCTGTTGT-3'.

Immunocytochemistry and immunohistochemistry

The surfaces of the cultured cells were washed three times with phosphate buffered saline (PBS) and the cells were fixed in 10% formalin for 10 min. After permeabilization with 0.5% Triton X-100 in PBS for 10 min, ameloblastin was stained using a polyclonal goat anti-ameloblastin antibody (1:50, Santa Cruz, Santa Cruz, CA, USA) for 1 h. After several washes with PBS containing 0.1% Tween 20 (Sigma, St. Louis, MO, USA), the cells were incubated with the secondary antibody, Alex-488-conjugated anti-goat IgG serum (1:200), for 1 h at room temperature. Nuclei were visualized by Hoechst 33258 (Wako, Osaka, Japan) staining. Confocal microscopy was performed using a Zeiss LSM 510 microscope (Carl Zeiss, Oberkochen, Germany).

Statistical Analysis

Result were presented as means ± standard deviation (n=3).SD. Date were statistically analyzed by Student t tests. $P < 0.05$ was regarded as significant.

Results

Interaction between epithelial and mesenchymal cells is important for tooth development. This interaction is mediated by the ECM, which acts as a cytokine store *in vivo*. It is therefore important to mimic ECM functions when constructing an *in vitro* co-culture system. We constructed two co-culture models to investigate the interaction between two different dental cell lines, a rat HAT-7 cell line that originated from dental epithelia, and bovine BCPb8 cells, derived from cementoblast progenitor cells (Fig. 1). One co-culture method, (sandwich co-culture; SW) cultured these cells by inoculation of the cell lines onto opposite sides of a collagen film suspended in a cell culture dish. The second, control method, termed "separate co-culture" (SC) cultured BCPb8 cells on the culture dish and the HAT-7 cells on a collagen film that faced away from the BCP8 cells on the dish.

To determine the gene expression levels of enamel matrix proteins quantitatively, we performed real-time PCR analysis using specific primers (Kurosawa et al. 2005). The specific rat primers used for this analysis were designed from regions of low-homology between rat and bovine cDNA to avoid cross-amplification. Glyceraldehyde-3-phosphate dehydrogenase mRNA expression in each cell line was used as an internal control. Ameloblastin mRNA expression in these culture systems is shown in Fig. 2. In the SW cells, the expression level of ameloblastin mRNA gradually increased after seeding of HAT-7 cells and continued to increase until at least day 14. The ameloblastin expression level was significantly increased on day 14 compared with the others condition such as SC culture, monolayer culture on a collagen membrane (ML). The degree of ameloblastin mRNA up-regulation in SC-cultured cells was less than that of SW-cultured cells on days 7 and 14. These results suggested that direct

interaction of HAT-7 and BCPb8 via the collagen membrane was important for tooth differentiation.

The expression of amelogenin mRNA in these culture systems is shown in Fig. 3. In the SW cells, the expression levels of amelogenin mRNA gradually increased after seeding of HAT-7 cells and continued to increase until at least day 14. On day 14, amelogenin expression was increased compared to HAT-7 cells grown in either monolayer culture or in SC method, although the difference compared to either control culture was not statistically significant. These results further suggest that direct interaction of HAT-7 and BCPb8 cells via a collagen membrane was important for tooth differentiation.

We next analyzed expression of the ameloblastin protein in the SW system by immunofluorescent staining using an anti-ameloblastin antibody, an Alexa 488-conjugated second antibody, and confocal laser scanning microscopy. The Alex488-Ameloblastin signal was detected in sandwich co-cultured HAT-7 cells from 3 days and had disappeared by day 14 (Fig. 4B, C and D). No ameloblastin signal was detected on day 1 of culture (Fig.4A). Ameloblastin protein expression was not detected in co-cultured BCPb8 cells on day 14 (Fig. 4E). These results indicate that HAT-7 cells can gradually differentiate into ameloblast-like cells in the SW system but not in the SC. These results suggest that interaction between HAT-7 and BCPb8 cells via a collagen membrane was important for tooth differentiation in protein expression level.

Discussion

We constructed and compared two *in vitro* culture systems both of which involved culture using a collagen membrane. Whereas, in both co-culture systems the two cell lines are exposed to soluble factors produced by both cell lines, only the SW co-culture system allows the two cell lines to physically contact each other through the collagen membrane. Our results showed that both the mRNA and protein expression of the ameloblastin were significantly increased in HAT-7 cells that were co-cultured with BCPb8 cells using the SW method. Soluble factors produced by the BCPb8 cells may also contribute to induction of ameloblastin expression. Furthermore, our data indicated that the collagen membrane might play a role, not only in the accumulation of, but also in the stabilization of, soluble factors from BCPb8 cells.

Although the soluble factors produced by BCPb8 cells that contribute to amelogenin expression have not been studied, they must be of relatively low molecular weight since only molecules with a molecular weight of less than 12.5 kDa can pass through the collagen membrane. Several soluble factors are known to be involved in the interaction between epithelial and mesenchymal tissue during tooth development including growth factors, cytokines and extracellular matrix molecules. Among these factors, the insulin-like growth factors (IGFs) have been proposed as autocrine/paracrine regulators of in vivo tooth development (Caton et al. 2005; Yamamoto et al. 2006) and the molecular weight of IGF is less than 12.5 kDa. Therefore, IGFs are promising candidate soluble factors for mediation of the stimulation of ameloblastin mRNA and protein expression in HAT-7 cells.

We reconstructed the interaction of dental epithelial and mesenchymal cells by co-culture of these cells using a collagen membrane *in vitro*. This method is easier to

perform than other methods of co-culture that use extracellular matrix components such as Matrigel. Using this method we were able to analyze cell signal transduction pathways that require dental epithelial and mesenchymal cell interactions. This study provides a useful tool for future analysis of epithelial-mesenchymal interactions.

Acknowledgments

This research was partially supported by the grant program "Collaborative Development of Innovative Seeds" from the Japan Science and Technology Agency (JST).

References

Aberg T, Wozney J, Thesleff I. 1997. Expression patterns of bone morphogenetic proteins (Bmps) in the developing mouse tooth suggest roles in morphogenesis and cell differentiation. Dev Dyn 210(4):383-96.

Caton J, Bringas P, Jr., Zeichner-David M. 2005. IGFs increase enamel formation by inducing expression of enamel mineralizing specific genes. Arch Oral Biol 50(2):123-9.

Cerny R, Slaby I, Hammarstrom L, Wurtz T. 1996. A novel gene expressed in rat ameloblasts codes for proteins with cell binding domains. J Bone Miner Res 11(7):883-91.

Fong CD, Slaby I, Hammarstrom L. 1996. Amelin: an enamel-related protein, transcribed in the cells of epithelial root sheath. J Bone Miner Res 11(7):892-8.

Fukumoto S, Kiba T, Hall B, Iehara N, Nakamura T, Longenecker G, Krebsbach PH, Nanci A, Kulkarni AB, Yamada Y. 2004. Ameloblastin is a cell adhesion molecule required for maintaining the differentiation state of ameloblasts. J Cell Biol 167(5):973-83.

Gingras M, Bergeron J, Dery J, Durham HD, Berthod F. 2003. In vitro development of a tissue-engineered model of peripheral nerve regeneration to study neurite growth. Faseb J 17(14):2124-6.

Hu CC, Fukae M, Uchida T, Qian Q, Zhang CH, Ryu OH, Tanabe T, Yamakoshi Y, Murakami C, Dohi N and others. 1997. Sheathlin: cloning, cDNA/polypeptide sequences, and immunolocalization of porcine enamel sheath proteins. J Dent Res 76(2):648-57.

Jernvall J, Keranen SV, Thesleff I. 2000. Evolutionary modification of development in mammalian teeth: quantifying gene expression patterns and topography. Proc Natl Acad Sci U S A 97(26):14444-8.

Kawano S, Morotomi T, Toyono T, Nakamura N, Uchida T, Ohishi M, Toyoshima K, Harada H. 2002. Establishment of dental epithelial cell line (HAT-7) and the cell differentiation dependent on Notch signaling pathway. Connect Tissue Res 43(2-3):409-12.

Krebsbach PH, Lee SK, Matsuki Y, Kozak CA, Yamada KM, Yamada Y. 1996. Full-length sequence, localization, and chromosomal mapping of ameloblastin. A novel tooth-specific gene. J Biol Chem 271(8):4431-5.

Kurosawa Y, Taniguchi A, Okano T. 2005. Novel method to examine hepatocyte-specific gene expression in a functional coculture system. Tissue Eng 11(11-12):1650-7.

Ohno M, Motojima K, Okano T, Taniguchi A. 2008. Up-regulation of drug-metabolizing enzyme genes in layered co-culture of a human liver cell line and endothelial cells. Tissue Eng Part A 14(11):1861-9.

Orisaka M, Mizutani T, Tajima K, Orisaka S, Shukunami K, Miyamoto K, Kotsuji F. 2006. Effects of ovarian theca cells on granulosa cell differentiation during gonadotropin-independent follicular growth in